

BEEDINGS, WEST SUSSEX OPTICAL DATING OF SEDIMENTARY DEPOSITS

SCIENTIFIC DATING REPORT

Phil Toms and Matthew Pope



BEEDINGS, WEST SUSSEX

OPTICAL DATING OF SEDIMENTARY DEPOSITS

Phil Toms and Matthew Pope

NGR: TQ 07410 20320

© English Heritage

ISSN 1749-8775

The Research Department Report Series incorporates reports from all the specialist teams within the English Heritage Research Department: Archaeological Science; Archaeological Archives; Historic Interiors Research and Conservation; Archaeological Projects; Aerial Survey and Investigation; Archaeological Survey and Investigation; Architectural Investigation; Imaging, Graphics and Survey, and the Survey of London. It replaces the former Centre for Archaeology Reports Series, the Archaeological Investigation Report Series and the Architectural Investigation Report Series.

Many of these are interim reports which make available the results of specialist investigations in advance of full publication. They are not usually subject to external refereeing, and their conclusions may sometimes have to be modified in the light of information not available at the time of the investigation. Where no final project report is available, readers must consult the author before citing these reports in any publication. Opinions expressed in Research Department reports are those of the author(s) and are not necessarily those of English Heritage.

Requests for further hard copies, after the initial print run, can be made by emailing:

Res.reports@english-heritage.org.uk

or by writing to:

English Heritage, Fort Cumberland, Fort Cumberland Road, Eastney, Portsmouth PO4 9LD

Please note that a charge will be made to cover printing and postage.

SUMMARY

Three OSL samples were taken from the main fissure investigated in Field 3. These have produced results entirely consistent with the current interpretation of site formation processes and technological elements at the site, and suggest that the entire process of fissure formation and in-filling was largely complete by the end of the last Glacial and that the lithics found within the fissure fill predate the Last Glacial Maximum and form part of Mousterian and Early Middle Palaeolithic assemblages. The work also proved the suitability of fissure contexts within the Lower Greensand to dating by OSL and the future potential for wide ranging dating programmes of fissure formation within the region.

CONTRIBUTORS

Dr Phil Toms (University of Gloucestershire) and Dr Matthew Pope (Archaeology South-East)

ACKNOWLEDGEMENTS

The OSL dating formed a part of The Beedings Survey, which is under the direction of Dr Matthew Pope (Archaeology South-East) and funded by English Heritage through the Historic Environment Commissions.

ARCHIVE LOCATION

Archaeology South-East, Centre for Applied Archaeology, Institute of Archaeology, University College London, 31–34 Gordon Square, London, WC1 0PY

DATE OF INVESTIGATION

2009

CONTACT DETAILS

Geochronology Laboratories, School of Natural and Social Sciences, University of Gloucestershire, Swindon Road, Cheltenham GL50 4AZ. Tel: 01242 714708
Email: ptoms@glos.ac.uk

CONTENTS

1.0 Introduction	1
2.0 Optical Dating: Mechanisms and Principles	4
3.0 Sample Collection and Preparation	4
4.0 Acquisition and Accuracy of D_e Value	5
4.1 Laboratory factors	6
4.1.1 Feldspar contamination	6
4.1.2 Preheating	6
4.1.3 Irradiation.....	7
4.1.4 Internal consistency	7
4.2 Environmental factors	8
4.2.1 Incomplete zeroing	8
4.2.2 Pedoturbation	9
5.0 Acquisition and Accuracy of D_r Value.....	9
6.0 Estimation of Age.....	10
7.0 Analytical Uncertainty.....	11
8.0 Results	12
9.0 Conclusion.....	12
10.0 References.....	13
Tables	16
Appendix 1: Technical Data for Sample GL08066.....	17
Appendix 2: Technical Data for Sample GL08067	18
Appendix 3: Technical Data for Sample GL08068.....	19

1.0 INTRODUCTION

The site of Beedings (NGR TQ0741020320) is situated in West Sussex on the edge of the Lower Greensand scarp 4km north-east of Pulborough (Fig 1). On the site is Beedings Castle, a monumental early 20th century house during the construction of which a series of underlying fissures were revealed within the underlying Greensand. These fissures were shown to contain a unique stone tool assemblage consisting of some 2,300 pieces of fresh, struck flint. Although much of the assemblage is now lost, enough remained for Jacobi (1986, 2007) to characterise it as the richest assemblage in Britain of the *Lincombian-Ransian-Jerzmanowician* industry (2007), an Early Upper Palaeolithic technology with a largely East European distribution. This industry is dated to 38–42ka, and the technology is currently thought by some researchers to be the product of the last Neanderthal hunting groups in this region.

In 2006, a threat to these nationally important stone artefact scatters emerged in the form of a land sale with subsequent ploughing and planting proposals scheduled for early 2008. The Beedings Survey was conceived to meet this threat directly and to begin the assessment of Heritage Management implications for other possible fissure sites elsewhere in south-east England. Fieldwork was undertaken in 2008 across the four fields that comprise Beedings Hill. During the course of the project the survey area was subjected to field walking and trench excavation. Across much of the landscape surveyed, evidence was found for multi-period occupation including Mesolithic flints, Late Iron Age pottery and Romano-British building material. In Field 3, adjacent to the original castle, artefact concentrations dating from the Lower Palaeolithic through to the Early Mesolithic were found in the loess-rich fill of fissures within the Lower Greensand. The Palaeolithic material includes both Mousterian (the first to be excavated *in situ* from southern Britain), and Early Upper Palaeolithic material. The latter is currently thought to represent the activities of the last Neanderthal hunting groups in northern Europe.

Three Optically Stimulated Luminescence (OSL) samples were taken from the main fissure investigated in Field 3 (Fig 2).

OSL sample BEED01 (Trench G) was taken at 0.24 cm depth immediately below the sub-soil, in order to provide a *terminus ante quem* for the main fissure fill.

OSL sample BEED02 (Trench G) was taken at 0.87m in the main artefact-bearing horizon of Early Upper Palaeolithic material within the fissure fill at this location. It therefore provides an age estimate for the sealing and final incorporation of these artefacts into the fissure and a *terminus ante quem* for their discard at the site.

OSL sample BEED03 (Trench F) was taken at 0.3m depth within the top of the fissure fill at this locality, at the same level which produced the bulk of Early Upper Palaeolithic artefacts and immediately above the level of Mousterian tools.

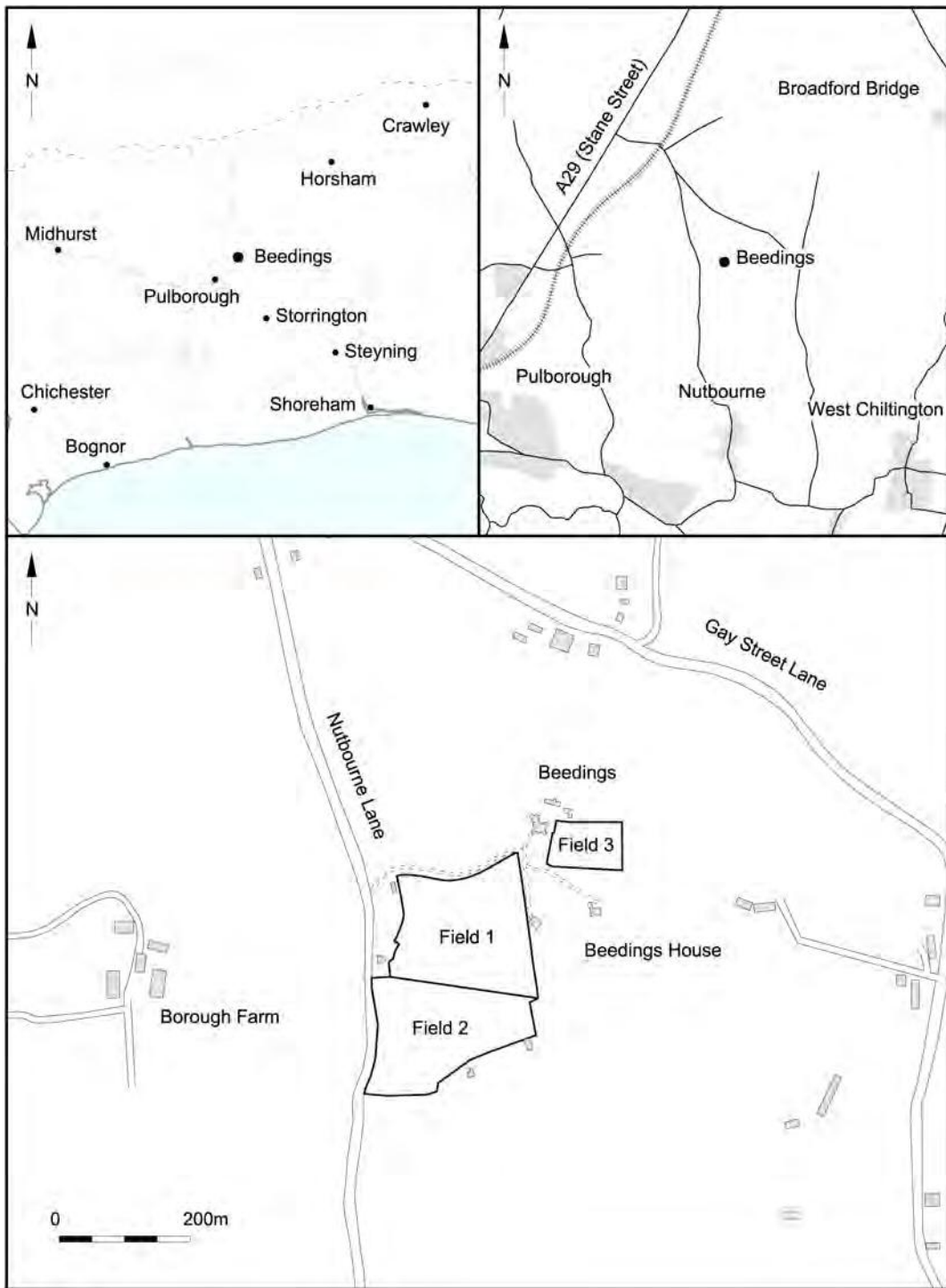


Figure 1. Study area for the Beedings site, near Pulborough

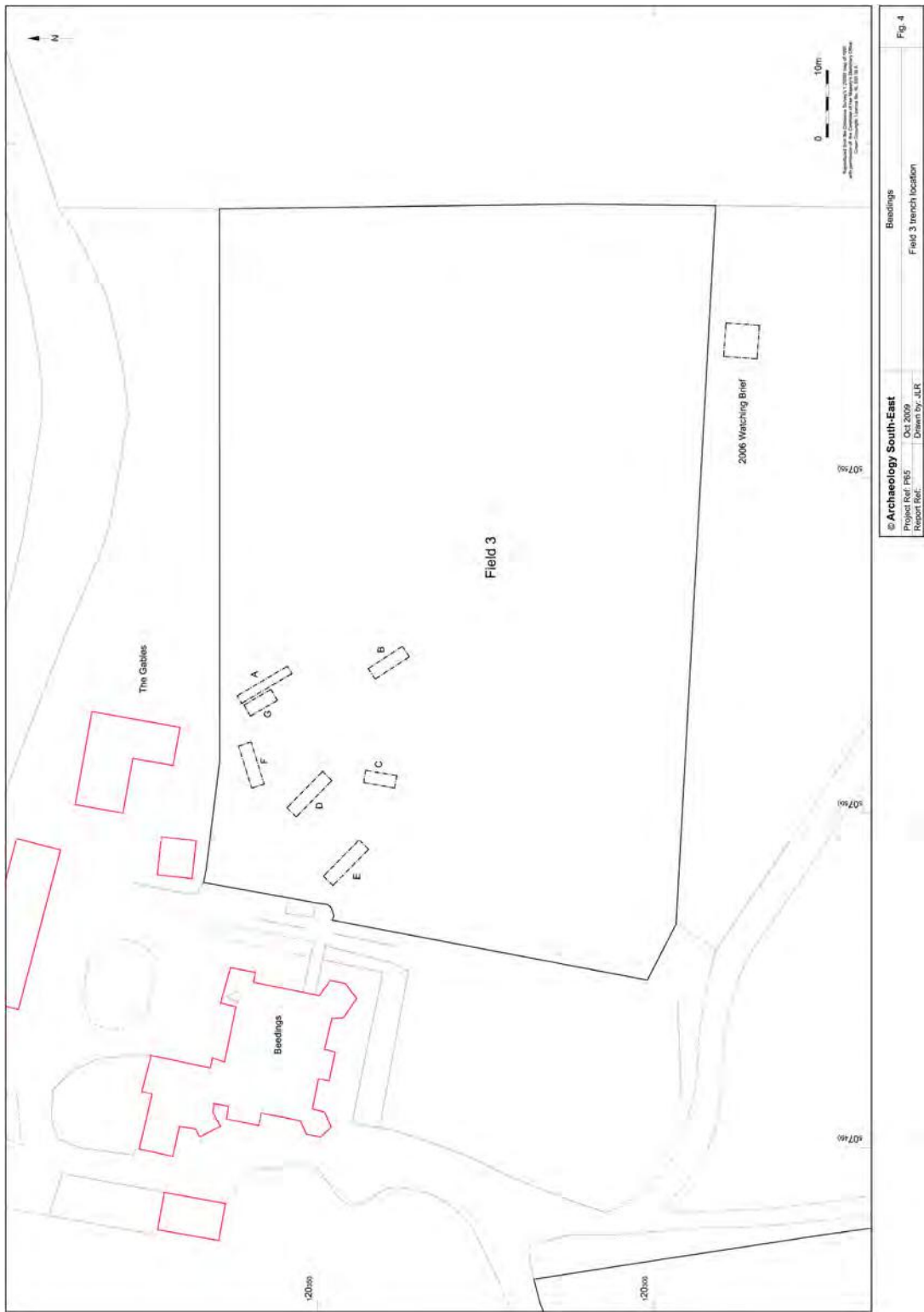


Figure 2. Field 3 at the Beedings site and locations for trenches F and G from which OSL samples were recovered

2.0 OPTICAL DATING: MECHANISMS AND PRINCIPLES

Upon exposure to ionising radiation, electrons within the crystal lattice of insulating minerals are displaced from their atomic orbits. Whilst this dislocation is momentary for most electrons, a portion of charge is redistributed to meta-stable sites (traps) within the crystal lattice. In the absence of significant optical and thermal stimuli, this charge can be stored for extensive periods. The quantity of charge relocation and storage relates to the magnitude and period of irradiation. When the lattice is optically or thermally stimulated, charge is evicted from traps and may return to a vacant orbit position (hole). Upon recombination with a hole, an electron's energy can be dissipated in the form of light-generating crystal luminescence, providing a measure of dose absorption.

Herein, quartz is segregated for dating. The utility of this minerogenic dosimeter lies in the stability of its datable signal over the mid to late Quaternary period, predicted through isothermal decay studies (eg Smith *et al* 1990; retention lifetime 630Ma at 20°C) and evidenced by optical age estimates concordant with independent chronological controls (eg Murray and Olley 2002). This stability is in contrast to the anomalous fading of comparable signals commonly observed for other ubiquitous sedimentary minerals, such as feldspar and zircon (Wintle 1973; Templer 1985; Spooner 1993).

Optical age estimates of sedimentation (Huntley *et al* 1985) are premised upon reduction of the minerogenic time-dependent signal (Optically Stimulated Luminescence, OSL) to zero through exposure to sunlight and, once buried, signal reformulation by absorption of litho- and cosmogenic radiation. The signal accumulated post-burial acts as a dosimeter recording total dose absorption, converting to a chronometer by estimating the rate of dose absorption quantified through the assay of radioactivity in the surrounding lithology and streaming from the cosmos.

$$\text{Age} = \text{Mean Equivalent Dose (D}_e\text{, Gy) / Mean Dose Rate (D}_r\text{, Gy.ka}^{-1}\text{)}$$

Aitken (1998) and Bøtter-Jensen *et al* (2003) offer a detailed review of optical dating.

3.0 SAMPLE COLLECTION AND PREPARATION

Three conventional sediment samples – those located within matrix-supported units composed predominantly of sand and silt – were collected in daylight from sections, by means of opaque plastic tubing (150x45mm) forced into each face. Each sample was wrapped in cellophane and parcel tape in order to preserve moisture content and integrity until ready for laboratory preparation. For each sample, an additional c 100g of sediment was collected for laboratory-based assessment of radioactive disequilibrium.

To preclude optical erosion of the datable signal prior to measurement, all samples were prepared under controlled laboratory illumination provided by Encapsulite RB-10 (red) filters. To isolate that material potentially exposed to daylight during sampling, sediment located within 20mm of each tube-end was removed.

Each Sample was subjected to acid and alkaline digestion (10% HCl, 15% H₂O₂) to attain removal of carbonate and organic components respectively. Quartz within fine silt (5–15µm) fraction was then segregated (Table 1).

Fine silt-sized quartz, along with other mineral grains of varying density and size, was extracted by sample sedimentation in acetone (<15µm in 2min 20s, >5µm in 21min at 20°C). Feldspars and amorphous silica were then removed from this fraction through acid digestion (35% H₂SiF₆ for two weeks, Jackson *et al* 1976; Berger *et al* 1980). Following addition of 10% HCl to remove acid-soluble fluorides, grains degraded to <5µm as a result of acid treatment were removed by acetone sedimentation. Twelve aliquots (c 1.5mg) were then mounted on aluminium discs for D_e evaluation.

All drying was conducted at 40°C to prevent thermal erosion of the signal. All acids and alkalis were Analar grade. All dilutions (removing toxic-corrosive and non-minerogenic luminescence-bearing substances) were conducted with distilled water to prevent signal contamination by extraneous particles.

4.0 ACQUISITION AND ACCURACY OF D_e VALUE

All minerals naturally exhibit marked inter-sample variability in luminescence per unit dose (sensitivity). Therefore, the estimation of D_e acquired since burial requires calibration of the natural signal using known amounts of laboratory dose. D_e values were quantified using a single-aliquot regenerative-dose (SAR) protocol (Murray and Wintle 2000; 2003) facilitated by a Risø TL-DA-15 irradiation-stimulation-detection system (Markey *et al* 1997; Bøtter-Jensen *et al* 1999). Within this apparatus, optical signal stimulation of each sample was provided by one of two light sources: an assembly of blue diodes (five packs of six Nichia NSPB500S), filtered to 470 ±80nm, conveying 15mW.cm⁻² using a 3mm Schott GG420 positioned in front of each diode pack. Infrared (IR) stimulation, provided by 6 IR diodes (Telefunken TSHA 6203) stimulating at 875 ±80nm delivering ~5mW.cm⁻², was used to indicate the presence of contaminant feldspars (Hütt *et al* 1988). Stimulated photon emissions from quartz aliquots are in the ultraviolet (UV) range and were filtered from stimulating photons by 7.5mm HOYA U-340 glass and detected by an EMI 9235QA photomultiplier fitted with a blue-green sensitive bialkali photocathode. Aliquot irradiation was conducted using a 1.48GBq ⁹⁰Sr/⁹⁰Y β source calibrated for multi-grain aliquots of 5–15µm quartz against the 'Hotspot 800' ⁶⁰Co γ source located at the National Physical Laboratory (NPL), UK.

SAR by definition evaluates D_e through measuring the natural signal (Fig 1 in each Appendix) of a single aliquot and then regenerating that aliquot's signal by using known laboratory doses to enable calibration. For each aliquot, five different regenerative doses were administered, so as to image dose response. D_e values for each aliquot were then interpolated, and associated counting and fitting errors calculated, by way of exponential plus linear regression (Fig 1 in each Appendix). Weighted (geometric) mean D_e values were calculated from the 12 aliquots using the central age model outlined by Galbraith *et*

al (1999), and are quoted at 1σ confidence. The accuracy with which D_e equates to total absorbed dose and that dose absorbed since burial was assessed. The former can be considered a function of laboratory factors, the latter, one of environmental issues. Diagnostics were deployed to estimate the influence of these factors and criteria instituted to optimise the accuracy of D_e values.

4.1 Laboratory factors

4.1.1 Feldspar contamination

The propensity of feldspar signals to fade and underestimate age, coupled with their higher sensitivity relative to quartz, makes it imperative to qualify feldspar contamination. At room temperature, feldspars generate a signal (IRSL) upon exposure to IR, whereas quartz does not (Fig 1 in each Appendix). The signal from feldspars contributing to OSL can be depleted by prior exposure to IR. For all aliquots the contribution of any remaining feldspars was estimated from the OSL IR depletion ratio (Duller 2003). If the addition to OSL by feldspars is insignificant, then the repeat dose ratio of OSL to post-IR OSL should be statistically consistent with unity. Any aliquots that did not fulfil this criterion were rejected. The source of feldspar contamination is rarely rooted in sample preparation; it predominantly results from the occurrence of feldspars as inclusions within quartz.

4.1.2 Preheating

Preheating aliquots between irradiation and optical stimulation is necessary to ensure comparability between natural and laboratory-induced signals. However, the multiple irradiation and preheating steps that are required to define single-aliquot regenerative-dose response leads to signal sensitisation, rendering calibration of the natural signal inaccurate. The SAR protocol (Murray and Wintle 2000; 2003) enables this sensitisation to be monitored and corrected using a test dose, here set at c 20Gy preheated to 220°C for 10s, to track signal sensitivity between irradiation-preheat steps. However, the accuracy of sensitisation correction for both natural and laboratory signals can be preheat-dependent. Three diagnostics were used to assess the optimal preheat temperature for accurate correction and calibration.

Irradiation-preheat cycling (Fig 2 in each Appendix) quantifies the preheat dependence of sensitisation correction for laboratory-induced signals. If sensitisation is accurately corrected, then the same regenerative dose should yield an equivalent sensitivity-corrected value, irrespective of the number of times it is applied and its associated signal measured. The ratio of subsequent to initial corrected regenerative-dose signals should be statistically concordant with unity. Alternatively, this ratio may differ from unity yet attain consistency after one or more cycles, evidencing that accurate sensitivity correction exists if the sample is primed by irradiation-preheat cycles. For this diagnostic, 18 aliquots were divided into sets of three, and assigned a 10s preheat between 180°C and 280°C.

D_e preheat dependence (Fig 3 in each Appendix) quantifies the combined effects of thermal transfer and sensitisation on the natural signal. Insignificant adjustment in D_e values in response to differing preheats may reflect limited influence of these effects. Samples generating D_e values $<10\text{Gy}$ and exhibiting a systematic, statistically significant adjustment in D_e value with increasing preheat temperature may indicate the presence of significant thermal transfer; in such instances low temperature ($<220^\circ\text{C}$) preheats may provide the apposite measure of D_e . For this diagnostic, the D_e value of each of the same 18 aliquots and their assigned preheat was assessed.

Dose recovery (Fig 4 in each Appendix) attempts to replicate the above diagnostic, yet provide improved resolution of thermal effects through removal of variability induced by heterogeneous dose absorption in the environment, using a precise laboratory dose to simulate natural dose. The ratio between the applied dose and recovered D_e value should be statistically concordant with unity. For this diagnostic, a further six aliquots were each assigned a 10s preheat between 180°C and 280°C .

That preheat treatment fulfilling the criterion of accuracy for all three diagnostics was selected to refine the final D_e value from a further nine aliquots. Further thermal treatments, prescribed by Murray and Wintle (2000; 2003), were applied to optimise accuracy and precision. Optical stimulation occurred at 125°C , in order to minimise effects associated with photo-transferred thermoluminescence and maximise signal-to-noise ratios. Inter-cycle optical stimulation was conducted at 280°C to minimise recuperation.

4.1.3 Irradiation

For all samples having D_e values in excess of 100Gy , matters of signal saturation and laboratory irradiation effects are of concern. As regards the former, the rate of signal accumulation generally adheres to a saturating exponential form, and it is this that limits the precision and accuracy of D_e values for samples having absorbed large doses. For such samples, the functional range of D_e interpolation is defined from log-linear plots of dose response. Within these plots, the maximum D_e value is delimited by the cessation of statistically significant increases in signal response. However, in this study no D_e value exceeded 100Gy .

4.1.4 Internal consistency

Quasi-radial plots (Fig 5 in each Appendix; cf Galbraith 1990) are used to illustrate inter-aliquot D_e variability for natural and regenerated signals. D_e values are standardised relative to the central D_e value for natural signals and applied dose for regenerated signals. D_e values are described as over-dispersed when $>5\%$ lie beyond $\pm 2\sigma$ of the standardising value, resulting from a heterogeneous absorption of burial dose and/or response to the SAR protocol. For multi-grain aliquots, over-dispersion for natural signals does not

necessarily imply inaccuracy. However, where over-dispersion is observed for regenerated signals, the age estimate for that sample should be accepted tentatively.

4.2 Environmental factors

4.2.1 Incomplete zeroing

Post-burial OSL signals residual of pre-burial dose absorption can result where pre-burial sunlight exposure is limited in spectrum, intensity, and/or period, leading to age over-estimation. This effect is particularly acute for material eroded and redeposited sub-aqueously (Olley *et al* 1998; 1999; Wallinga 2002) and exposed to a burial dose of <20Gy (eg Olley *et al* 2004) and can have some influence in sub-aerial contexts, but is rarely of consequence where aerial transport has occurred. Within single-aliquot regenerative-dose optical dating, there are two diagnostics of partial resetting (or bleaching); signal analysis (Agersnap Larsen *et al* 2000; Bailey *et al* 2003) and inter-aliquot D_e distribution studies (Murray *et al* 1995).

Within this study, signal analysis is used to quantify the change in D_e value with respect to optical stimulation time for multi-grain aliquots. This exploits the existence of traps within minerogenic dosimeters that bleach with different efficiency for a given wavelength of light to verify partial bleaching. $D_e(t)$ plots (Fig 6 in each Appendix; Bailey *et al* 2003) are constructed from separate integrals of signal decay as laboratory optical stimulation progresses. A statistically significant increase in natural $D_e(t)$ is indicative of partial bleaching, assuming three conditions are fulfilled. Firstly, that a statistically significant increase in $D_e(t)$ is observed when partial bleaching is simulated within the laboratory. Secondly, that there is no significant rise in $D_e(t)$ when full bleaching is simulated. Finally, there should be no significant augmentation in $D_e(t)$ when zero dose is simulated. Where partial bleaching is detected, the age derived from the sample should be considered a maximum estimate only. However, the utility of signal analysis is strongly dependent upon a sample's pre-burial experience of sunlight's spectrum and its residual to post-burial signal ratio. Given that, in the majority of cases, the spectral exposure history of a deposit is uncertain, the absence of an increase in natural $D_e(t)$ does not necessarily testify to the absence of partial bleaching.

Where requested and feasible, the insensitivities of multi-grain single-aliquot signal analysis may be circumvented by inter-aliquot D_e distribution studies. This analysis uses aliquots of single sand grains to quantify inter-grain D_e distribution. At present, it is contended that asymmetric inter-grain D_e distributions are symptomatic of partial bleaching and/or pedoturbation (Murray *et al* 1995; Olley *et al* 1999; 2004; Bateman *et al* 2003). For partial bleaching at least, it is further contended that the D_e acquired during burial is located in the minimum region of such ranges. The mean and breadth of this minimum region is the subject of current debate, as it is additionally influenced by heterogeneity in microdosimetry, variable inter-grain response to SAR, and residual to post-burial signal ratios. Presently, the apposite measure of age is that defined by the D_e interval delimited

by the minimum and central age models of Galbraith *et al* (1999). Single grain analysis was not requested, nor is feasible in the present study given the dearth of fine sand grains.

4.2.2 Pedoturbation

The accuracy of sedimentation ages can further be affected by post-burial trans-strata grain movements forced by pedo- or cryoturbation. Berger (2003) contends that pedogenesis prompts a reduction in the apparent sedimentation age of parent material through bioturbation and illuviation of younger material from above, and/or by biological recycling and resetting of the datable signal of surface material. Berger (2003) proposes that the chronological products of this remobilisation are A-horizon age estimates reflecting the cessation of pedogenic activity, Bc/C-horizon ages delimiting the maximum age for the initiation of pedogenesis, with estimates obtained from Bt-horizons providing an intermediate age 'close to the age of cessation of soil development'. Singhvi *et al* (2001), in contrast, suggest that B and C-horizons closely approximate the age of the parent material, the A-horizon, that of the 'soil forming episode'. At present there is no post-sampling mechanism for the direct detection of, and correction for, post-burial sediment remobilisation. However, intervals of palaeosol evolution can be delimited by a maximum age derived from parent material and a minimum age obtained from a unit overlying the palaeosol. Inaccuracy forced by cryoturbation may be bidirectional, heaving older material upwards or drawing younger material downwards into the level to be dated. Cryogenic deformation of matrix-supported material is, typically, visible; sampling of such cryogenically-disturbed sediments can be avoided.

5.0 ACQUISITION AND ACCURACY OF D_r VALUE

Lithogenic D_r values were defined through measurement of U, Th, and K radionuclide concentration, and conversion of these quantities into α , β , and γ D_r values (Table 1). α and β contributions were estimated from sub-samples by laboratory-based γ spectrometry using an Ortec GEM-S high purity Ge coaxial detector system, calibrated using certified reference materials supplied by CANMET. γ dose rates were estimated from *in-situ* NaI gamma spectrometry. *In-situ* measurements were conducted using an EG&G μ Nomad portable NaI gamma spectrometer (calibrated using the block standards at RLAHA, University of Oxford); these reduce uncertainty relating to potential heterogeneity in the γ dose field surrounding each sample. The level of U disequilibrium was estimated by laboratory-based Ge γ spectrometry. Estimates of radionuclide concentration were converted into D_r values (Adamiec and Aitken 1998), accounting for D_r modulation forced by grain size (Mejdahl 1979), present moisture content (Zimmerman 1971), and, given that D_e values were generated from 5–15 μ m quartz, reduced signal sensitivity to α radiation (a-value 0.050 \pm 0.002; Toms unpubl data). Cosmogenic D_r values are calculated on the basis of sample depth, geographical position, and matrix density (Prescott and Hutton 1994).

The spatiotemporal validity of D_r values can be considered as five variables. Firstly, age estimates devoid of *in-situ* γ spectrometry data should be accepted tentatively if the sampled unit is heterogeneous in texture or if the sample is located within 0.3m of strata consisting of differing texture and/or mineralogy. However, where samples are obtained throughout a vertical profile, consistent values of γD_r based solely on laboratory measurements may evidence the homogeneity of the γ field and hence accuracy of γD_r values. Secondly, disequilibrium can force temporal instability in U and Th emissions. The impact of this infrequent phenomenon (Olley *et al* 1996) upon age estimates is usually insignificant, given their associated margins of error. However, for samples where this effect is pronounced (>50% disequilibrium between ^{238}U and ^{226}Ra ; Fig 7 in each Appendix), the resulting age estimates should be accepted tentatively. Thirdly, pedogenically-induced variations in matrix composition of B and C-horizons, such as radionuclide and/or mineral remobilisation, may alter the rate of energy emission and/or absorption. If D_r is invariant through a dated profile and samples encompass primary parent material, then element mobility is probably limited in effect. In this study, there is limited evidence of pedogenesis for any unit sampled. Fourthly, spatiotemporal deviations from present moisture content are difficult to assess directly, requiring knowledge of the magnitude and timing of differing contents. However, the maximum influence of moisture content variations can be delimited by recalculating D_r for minimum (zero) and maximum (saturation) content. Finally, temporal alteration in the thickness of overburden alters cosmic D_r values. Cosmic D_r often forms a negligible portion of total D_r . It is possible to quantify the maximum influence of overburden flux by recalculating D_r for minimum (zero) and maximum (surface sample) cosmic D_r .

6.0 ESTIMATION OF AGE

Age estimates reported in Table 1 provide an estimate of sediment burial period based on mean D_e and D_r values and their associated analytical uncertainties. Uncertainty in age estimates is reported as a product of systematic and experimental errors, with the magnitude of experimental errors alone shown in parentheses (Table 1). Probability distributions indicate the inter-aliquot variability in age (Fig 8 in each Appendix). The maximum influence of temporal variations in D_r forced by minima-maxima variation in moisture content and overburden thickness is illustrated in Figure 8 in each Appendix. Where uncertainty in these parameters exists, this age range may prove instructive, but the combined extremes represented should not be construed as preferred age estimates.

7.0 ANALYTICAL UNCERTAINTY

All errors are based upon analytical uncertainty and quoted at 1σ confidence. Error calculations account for the propagation of systematic and/or experimental (random) errors associated with D_e and D_r values.

For D_e values, systematic errors are confined to laboratory β source calibration. Uncertainty in this respect is that combined from the delivery of the calibrating γ dose (1.2%; NPL pers comm), the conversion of this dose for SiO_2 using the respective mass energy-absorption coefficient (2%; Hubbell 1982) and experimental error, totalling 3.5%. Mass attenuation and Bremsstrahlung losses during γ dose delivery are considered negligible. Experimental errors relate to D_e interpolation using sensitisation-corrected dose responses. Natural and regenerated sensitisation corrected dose points (S_i) are quantified by

$$S_i = (D_i - x.L_i) / (d_i - x.L_i) \quad \text{Eq. 1}$$

where D_i = Natural or regenerated OSL, initial 0.2s

L_i = Background natural or regenerated OSL, final 5s

d_i = Test dose OSL, initial 0.2s

x = Scaling factor, 0.08

The error on each signal parameter is based on counting statistics, reflected by the square-root of measured values. The propagation of these errors within Eq. 1 generating σS_i follows the general formula given in Eq. 2. σS_i are then used to define fitting and interpolation errors within linear or exponential regressions (Green and Margerison 1978; Ixaru and Vanden Berghe 2004).

For D_r values, systematic errors accommodate uncertainty in radionuclide conversion factors (5%), β attenuation coefficients (5%), a -value (4%; derived from a systematic α source uncertainty of 3.5% and experimental error), matrix density (0.20 g.cm^{-3}), vertical thickness of sampled section (specific to sample collection device), saturation moisture content (3%), moisture content attenuation (2%), burial moisture content (25% relative, unless direct evidence exists of the magnitude and period of differing content), NaI gamma spectrometer calibration (3%) and/or NAA/ICP-MS (2%). Experimental errors are associated with radionuclide quantification for each sample by gamma spectrometry and/or NAA/ICP-MS.

The propagation of these errors through to age calculation is quantified using the expression,

$$\sigma_y (\delta y / \delta x) = (\sum ((\delta y / \delta x_n) \cdot \sigma_{x_n})^2)^{1/2} \quad \text{Eq. 2}$$

where y is a value equivalent to that function comprising terms x_n and where σ_y and σ_{x_n} are associated uncertainties.

Errors on age estimates are presented as combined systematic and experimental errors and experimental errors alone. The former (combined) error should be considered when comparing luminescence ages herein with independent chronometric controls. The latter assumes systematic errors are common to luminescence age estimates generated by means equal to those detailed herein and enable direct comparison with those estimates.

8.0 RESULTS

Individual sample details are given in Table I, while the technical details for each sample are given in Appendix I–III. The summary of the results follows:

Sample BEED01 (GL08066) gives a date of 16,000 ± 1000 years (before sampling date; 2008) for the top of the fissure fill immediately below the sub-soil. This indicates that the main fissure was effectively sealed to the modern landsurface during the Last Glacial Maximum. These processes combined to form the overlying subsoil.

Sample BEED02 (GL08067) gives a date of 31,000 ± 2000 years for the main artefact-bearing horizon. It indicates that artefacts were discarded at the site before this date and finally sealed within fissure sediments beyond bioturbation and later disturbance by this date.

Sample BEED03 (GL08068) gives an age estimate of 30,000 ± 1000 years for the incorporation of Early Upper Palaeolithic artefacts within the main fissure fill at Trench F. This is consistent with the date for the same horizon at Trench G and also provides a *terminus ante quem* for more deeply stratified Mousterian artefacts found within this fissure.

9.0 CONCLUSION

The dating programme has produced results entirely consistent with our current interpretation of site formation processes and technological elements at the site. It suggests that the entire process of fissure formation and in-filling was largely complete by the end of the last Glacial and that the lithics found within the fissure fill predate the Last Glacial Maximum and form part of Mousterian and Early Middle Palaeolithic assemblages. The work also proved the suitability of fissure contexts within the Lower Greensand to dating by OSL and the future potential for wide ranging dating programmes of fissure in-filling within the region.

10.0 REFERENCES

- Adamiec, G, and Aitken, M J, 1998 Dose-rate conversion factors: new data, *Ancient TL*, **16**, 37–50
- Agersnap Larsen, N, Bulur, E, Bøtter-Jensen, L, and McKeever, S W S, 2000 Use of the LM-OSL technique for the detection of partial bleaching in quartz, *Radiation Measurements*, **32**, 419–25.
- Aitken, M J, 1998 *An Introduction to Optical Dating: the Dating of Quaternary Sediments by the Use of Photon-Stimulated Luminescence*, Oxford (Oxford Univ Press)
- Bailey, R M, Singarayer, J S, Ward, S, and Stokes, S, 2003 Identification of partial resetting using D_e as a function of illumination time, *Radiation Measurements*, **37**, 511–18
- Bateman, M D, Frederick, C D, Jaiswal, M K, and Singhvi, A K, 2003 Investigations into the potential effects of pedoturbation on luminescence dating, *Quaternary Sci Rev*, **22**, 1169–76
- Berger, G W, 2003 Luminescence chronology of late Pleistocene loess-paleosol and tephra sequences near Fairbanks, Alaska, *Quat Res*, **60**, 70–83
- Bøtter-Jensen, L, Mejdahl, V, and Murray, A S, 1999 New light on OSL, *Quat Sci Rev*, **18**, 303–10
- Bøtter-Jensen, L, McKeever, S W S, and Wintle, A G, 2003 *Optically Stimulated Luminescence Dosimetry*, Amsterdam (Elsevier)
- Duller, G A T, 2003 Distinguishing quartz and feldspar in single grain luminescence measurements, *Radiation Measurements*, **37**, 161–5.
- Galbraith, R F 1990 The radial plot: graphical assessment of spread in ages. *Nuclear Tracks and Radiation Measurements*, **17**, 207–14
- Galbraith, R F, Roberts, R G, Laslett, G M, Yoshida, H, and Olley, J M, 1999 Optical dating of single and multiple grains of quartz from Jinmium rock shelter (northern Australia): Part I, Experimental design and statistical models, *Archaeometry*, **41**, 339–64
- Green, J R and Margerison, D, 1978 *Statistical Treatment of Experimental Data*, New York (Elsevier Scientific Publications)
- Hubble, J H, 1982 Photon mass attenuation and energy-absorption coefficients from 1 keV to 20 MeV, *Int J Applied Radioisotopes*, **33**, 1269–90

Huntley, D J, Godfrey-Smith, D I, and Thewalt, M L W, 1985 Optical dating of sediments, *Nature*, **313**, 105–7

Hütt, G, Jaek, I, and Tchonka, J, 1988 Optical dating: K-feldspars optical response stimulation spectra, *Quaternary Sci Rev*, **7**, 381–6

Ixaru, L, and Vanden Berghe, G, 2004 *Exponential Fitting*, Dordrecht (Kluwer Academic Press)

Jacobi, R M, 1986 The contents of Dr Harley's show case, in S N Collcutt (ed), *The Palaeolithic of Britain and its Nearest Neighbours: recent trends*, Sheffield (University of Sheffield, Department of Archaeology and Prehistory: John R Collis), 62–8

Jacobi, R M, 2007 An Early Upper Palaeolithic Assemblage from Beedings, near Pulborough, West Sussex, *Proc Prehist Soc*, **73**, 229–325

Markey, B G, Bøtter-Jensen, L, and Duller, G A T, 1997 A new flexible system for measuring thermally and optically stimulated luminescence, *Radiation Measurements*, **27**, 83–9

Mejdahl, V, 1979 Thermoluminescence dating: beta-dose attenuation in quartz grains, *Archaeometry*, **21**, 61–72

Murray, A S and Olley, J M, 2002 Precision and accuracy in the Optically Stimulated Luminescence dating of sedimentary quartz: a status review, *Geochronometria*, **21**, 1–16

Murray, A S and Wintle, A G, 2000 Luminescence dating of quartz using an improved single-aliquot regenerative-dose protocol, *Radiation Measurements*, **32**, 57–73

Murray, A S and Wintle, A G, 2003 The single aliquot regenerative dose protocol: potential for improvements in reliability. *Radiation Measurements*, **37**, 377–81

Murray, A S, Olley, J M, and Caitcheon, G G, 1995 Measurement of equivalent doses in quartz from contemporary water-lain sediments using optically stimulated luminescence, *Quaternary Sci Rev*, **14**, 365–71

Olley, J M, Murray, A S, and Roberts, R G, 1996 The effects of disequilibria in the Uranium and Thorium decay chains on burial dose rates in fluvial sediments. *Quaternary Sci Rev*, **15**, 751–60

Olley, J M, Caitcheon, G G, and Murray, A S, 1998 The distribution of apparent dose as determined by optically stimulated luminescence in small aliquots of fluvial quartz: implications for dating young sediments, *Quat Sci Rev*, **17**, 1033–40

- Olley, J M, Caitcheon, G G, and Roberts R G, 1999 The origin of dose distributions in fluvial sediments, and the prospect of dating single grains from fluvial deposits using - optically stimulated luminescence, *Radiation Measurements*, **30**, 207–17
- Olley, J M, Pietsch, T, and Roberts, R G, 2004 Optical dating of Holocene sediments from a variety of geomorphic settings using single grains of quartz, *Geomorphol*, **60**, 337–58
- Prescott, J R and Hutton, J T, 1994 Cosmic ray contributions to dose rates for luminescence and ESR dating: large depths and long-term time variations, *Radiation Measurements*, **23**, 497–500
- Singhvi, A K, Bluszcz, A, Bateman, M D, and Someshwar Rao, M, 2001 Luminescence dating of loess-palaeosol sequences and coversands: methodological aspects and palaeoclimatic implications, *Earth Sci Rev*, **54**, 193–211
- Smith, B W, Rhodes, E J, Stokes, S, and Spooner, N A, 1990 The optical dating of sediments using quartz, *Radiation Protection Dosimetry*, **34**, 75–8
- Spooner, N A, 1993 'The validity of optical dating based on feldspar', unpubl DPhil thesis, Oxford Univ
- Templer, R H, 1985 The removal of anomalous fading in zircons, *Nuclear Tracks and Radiation Measurements*, **10**, 531–7
- Wallinga, J, 2002 Optically stimulated luminescence dating of fluvial deposits: a review, *Boreas*, **31**, 303–22
- Wintle, A G, 1973 Anomalous fading of thermoluminescence in mineral samples, *Nature*, **245**, 143–4
- Zimmerman, D W, 1971 Thermoluminescent dating using fine grains from pottery, *Archaeometry*, **13**, 29–52

TABLES

Field Code		BEED01	BEED02	BEED03
Lab Code		GL08066	GL08067	GL08068
Location		51°N, 0°W, 85 m	51°N, 0°W, 85 m	51°N, 0°W, 85 m
Overburden (m)		0.24	0.87	0.3
Grain size (µm)		5–15	5–15	5–15
Moisture content		0.14 ± 0.03	0.16 ± 0.04	0.13 ± 0.03
NaI γ-spectrometry (in situ)	K (%)	0.68 ± 0.02	0.77 ± 0.02	0.70 ± 0.03
	Th (ppm)	5.20 ± 0.19	6.01 ± 0.20	5.87 ± 0.23
	U (ppm)	2.82 ± 0.13	2.92 ± 0.13	2.46 ± 0.15
γ D _r (Gy.ka ⁻¹)		0.73 ± 0.03	0.80 ± 0.03	0.73 ± 0.03
Ge γ-spectrometry (lab based)	K (%)	1.00 ± 0.05	1.02 ± 0.05	1.09 ± 0.05
	Th (ppm)	7.71 ± 0.50	7.99 ± 0.50	8.49 ± 0.52
	U (ppm)	1.74 ± 0.10	1.95 ± 0.10	1.80 ± 0.10
α D _r (Gy.ka ⁻¹)		0.34 ± 0.03	0.36 ± 0.04	0.37 ± 0.03
β D _r (Gy.ka ⁻¹)		1.04 ± 0.08	1.06 ± 0.09	1.14 ± 0.08
Cosmic D _r (Gy.ka ⁻¹)		0.20 ± 0.03	0.18 ± 0.02	0.20 ± 0.03
Total D _r (Gy.ka ⁻¹)		2.32 ± 0.10	2.40 ± 0.10	2.44 ± 0.10
Preheat (°C for 10s)		220	280	260
De (Gy)		38.2 ± 2.0	73.8 ± 4.2	72.7 ± 6.7
Age (ka)		16 ± 1 (1)	31 ± 2 (2)	30 ± 3 (3)

Table 1 D_r, D_e and Age data of submitted samples. Uncertainties in age are quoted at 1σ confidence, are based on analytical errors and reflect combined systematic and experimental variability and (in parentheses) experimental variability alone (see 7.0). Blue indicates samples with accepted age estimates; red, age estimates with caveats (see Table 2)

Generic considerations	Field Code	Lab Code	Sample-specific considerations
None	BEED01	GL08066	Overdispersion of regenerative-dose data; accept tentatively (see 4.1.4)
	BEED02	GL08067	None
	BEED03	GL08068	None

Table 2 Validity of sample suite age estimates and caveats for consideration

APPENDIX I: TECHNICAL DATA FOR SAMPLE GL08066

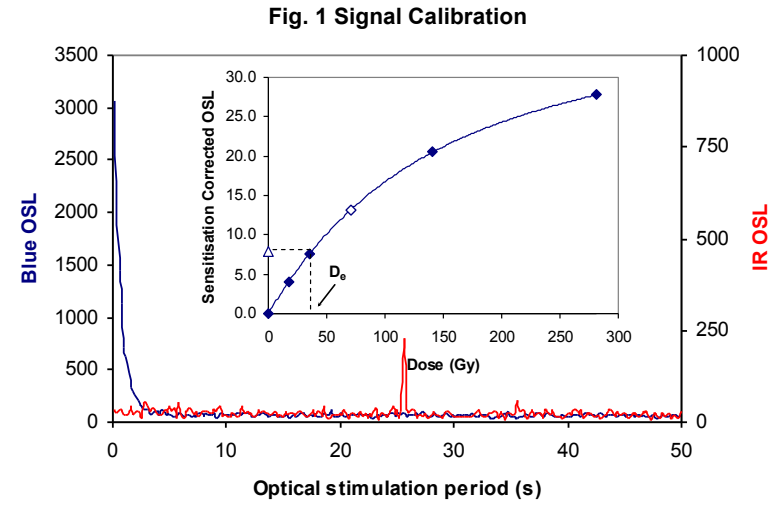


Fig. 1 Signal Calibration Natural blue and laboratory-induced infrared (IR) OSL signals. Detectable IR signal decays are diagnostic of feldspar contamination. Inset, the natural blue OSL signal (open triangle) of each aliquot is calibrated against known laboratory doses to yield equivalent dose (D_e) values. Where D_e values are $>100\text{Gy}$, a log-linear plot of dose response is shown; D_e can be confidently interpolated if signal response increases with dose.

Fig. 2 Irradiation-Preheat Cycling The acquisition of D_e values is necessarily predicated upon thermal treatment of aliquots succeeding environmental and laboratory irradiation. Repeated irradiation and thermal treatment results in aliquot sensitisation, rendering calibration of the natural signal inaccurate. This sensitisation can be monitored and corrected for. The accuracy of correction can be preheat dependent; irradiation-preheat cycling quantifies this dependence for laboratory-induced signals, examining the reproducibility of corrected OSL resultant of repeat laboratory doses. The significance of feldspar contamination can be quantified by measuring the post-IR blue repeat ratio (open symbol).

Fig. 3 D_e Preheat Dependence Quantifies the combined effects of thermal transfer and sensitisation on the natural signal. Insignificant adjustment in D_e may reflect limited influence of these effects

Fig. 4 Dose Recovery Attempts to replicate the above diagnostic, yet provide improved resolution of thermal effects through removal of variability induced by heterogeneous dose absorption in the environment and using a precise lab dose to simulate natural dose. Based on this and preceding data an appropriate thermal treatment is selected to refine the final D_e value.

Fig. 5 Inter-aliquot D_e distribution Provides a measure of inter-aliquot statistical concordance in D_e values derived from natural and laboratory irradiation. Discordant data (those points lying beyond ± 2 standardised $\ln D_e$) reflects heterogeneous dose absorption and/or inaccuracies in calibration.

Fig. 6 Signal Analysis Statistically significant increase in natural D_e value with signal stimulation period is indicative of a partially-bleached signal, provided a significant increase in D_e results from simulated partial bleaching along with insignificant adjustment in D_e for simulated zero and full bleach conditions. Ages from such samples are considered maximum estimates.

Fig. 7 U Activity Statistical concordance (equilibrium) in the activities of the daughter radioisotope ^{226}Ra with its parent ^{238}U may signify the temporal stability of D_e emissions from these chains. Significant differences (disequilibrium; $>50\%$) in activity indicate addition or removal of isotopes creating a time-dependent shift in D_e values and increased uncertainty in the accuracy of age estimates. 20% disequilibrium marker is also shown.

Fig. 8 Age Range The mean age range provides an estimate of sediment burial period based on mean D_e and D_e values with associated analytical uncertainties. The probability distribution indicates the inter-aliquot variability in age. The maximum influence of temporal variations in D_e forced by minima-maxima variation in moisture content and overburden thickness may prove instructive where there is uncertainty in these parameters, however the combined extremes represented should not be construed as preferred age estimates.

Fig. 2 Irradiation-Preheat Cycling

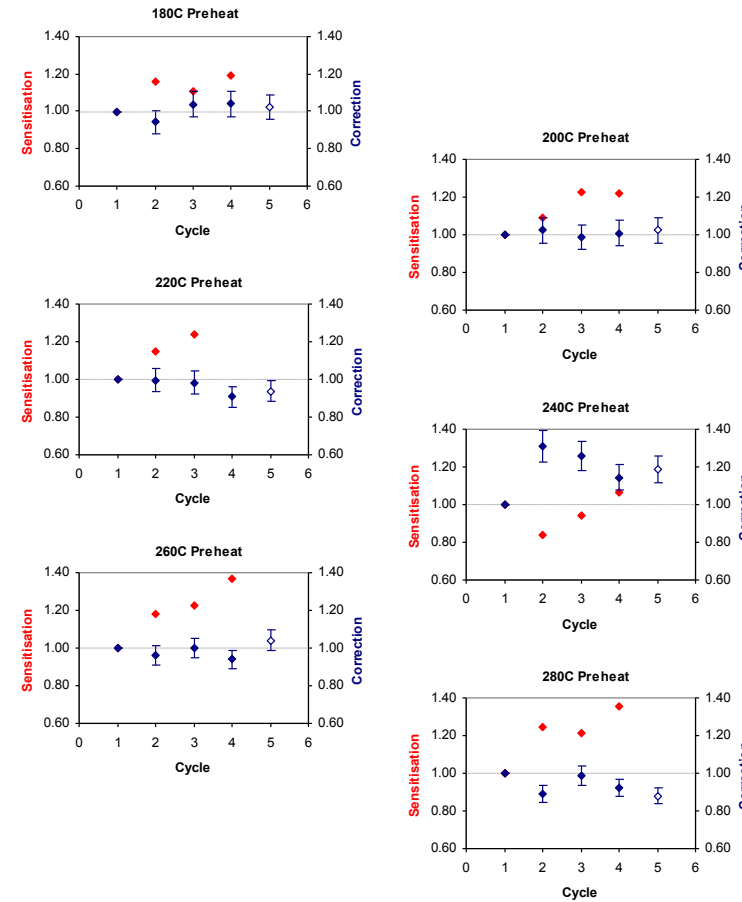


Fig. 3 D_e Preheat Dependence

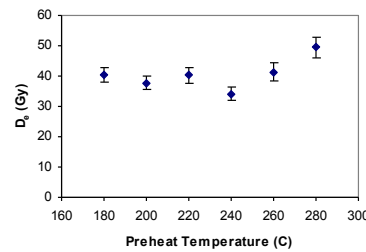


Fig. 4 Dose Recovery

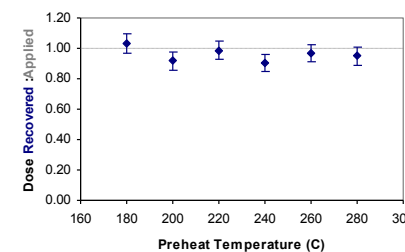


Fig. 5 Inter-aliquot D_e distribution

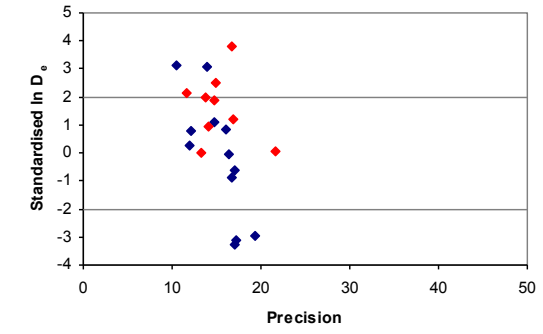


Fig. 6 Signal Analysis

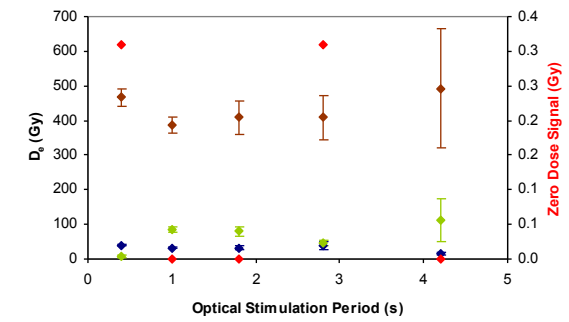


Fig. 7 U Decay Activity

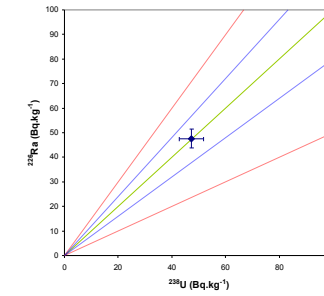
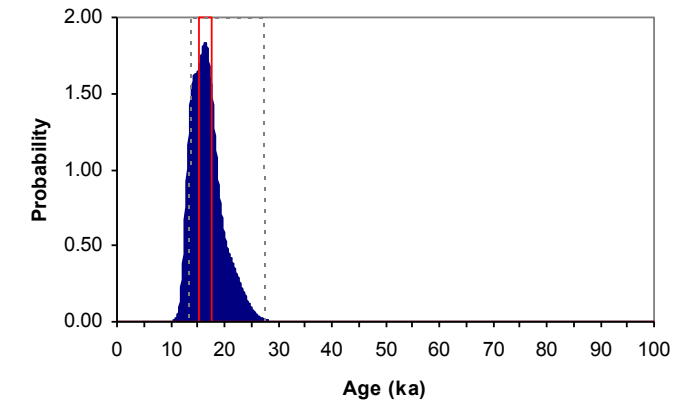


Fig. 8 Age Range



Sample: GL08066

APPENDIX 2: TECHNICAL DATA FOR SAMPLE GL08067

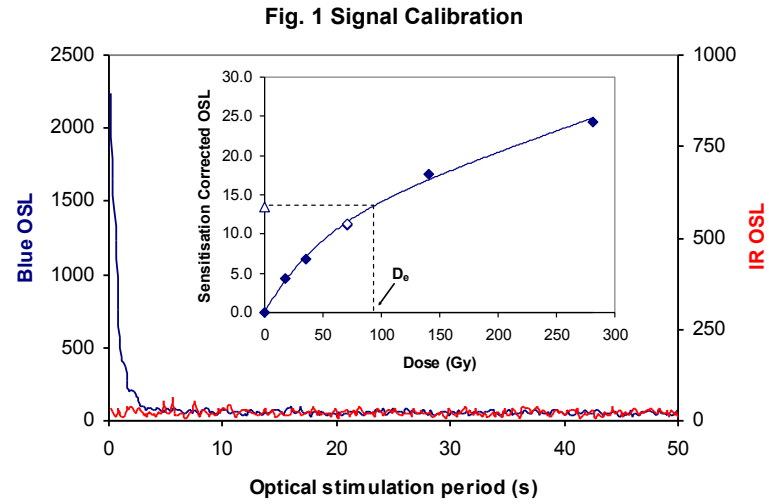


Fig. 1 Signal Calibration Natural blue and laboratory-induced infrared (IR) OSL signals. Detectable IR signal decays are diagnostic of feldspar contamination. Inset, the natural blue OSL signal (open triangle) of each aliquot is calibrated against known laboratory doses to yield equivalent dose (D_e) values. Where D_e values are >100Gy, a log-linear plot of dose response is shown; D_e can be confidently interpolated if signal response increases with dose.

Fig. 2 Irradiation-Preheat Cycling The acquisition of D_e values is necessarily predicated upon thermal treatment of aliquots succeeding environmental and laboratory irradiation. Repeated irradiation and thermal treatment results in aliquot sensitisation, rendering calibration of the natural signal inaccurate. This sensitisation can be monitored and corrected for. The accuracy of correction can be preheat dependent; irradiation-preheat cycling quantifies this dependence for laboratory-induced signals, examining the reproducibility of corrected OSL resultant of repeat laboratory doses. The significance of feldspar contamination can be quantified by measuring the post-IR blue repeat ratio (open symbol).

Fig. 3 D_e Preheat Dependence Quantifies the combined effects of thermal transfer and sensitisation on the natural signal. Insignificant adjustment in D_e may reflect limited influence of these effects

Fig. 4 Dose Recovery Attempts to replicate the above diagnostic, yet provide improved resolution of thermal effects through removal of variability induced by heterogeneous dose absorption in the environment and using a precise lab dose to simulate natural dose. Based on this and preceding data an appropriate thermal treatment is selected to refine the final D_e value.

Fig. 5 Inter-aliquot D_e distribution Provides a measure of inter-aliquot statistical concordance in D_e values derived from natural and laboratory irradiation. Discordant data (those points lying beyond ± 2 standardised in D_e) reflects heterogeneous dose absorption and/or inaccuracies in calibration.

Fig. 6 Signal Analysis Statistically significant increase in natural D_e value with signal stimulation period is indicative of a partially-bleached signal, provided a significant increase in D_e results from simulated partial bleaching along with insignificant adjustment in D_e for simulated zero and full bleach conditions. Ages from such samples are considered maximum estimates.

Fig. 7 U Activity Statistical concordance (equilibrium) in the activities of the daughter radioisotope ^{226}Ra with its parent ^{238}U may signify the temporal stability of D_e emissions from these chains. Significant differences (disequilibrium; >50%) in activity indicate addition or removal of isotopes creating a time-dependent shift in D_e values and increased uncertainty in the accuracy of age estimates. 20% disequilibrium marker is also shown.

Fig. 8 Age Range The mean age range provides an estimate of sediment burial period based on mean D_e and D_e values with associated analytical uncertainties. The probability distribution indicates the inter-aliquot variability in age. The maximum influence of temporal variations in D_e forced by minima-maxima variation in moisture content and overburden thickness may prove instructive where there is uncertainty in these parameters, however the combined extremes represented should not be construed as preferred age estimates.

Fig. 2 Irradiation-Preheat Cycling

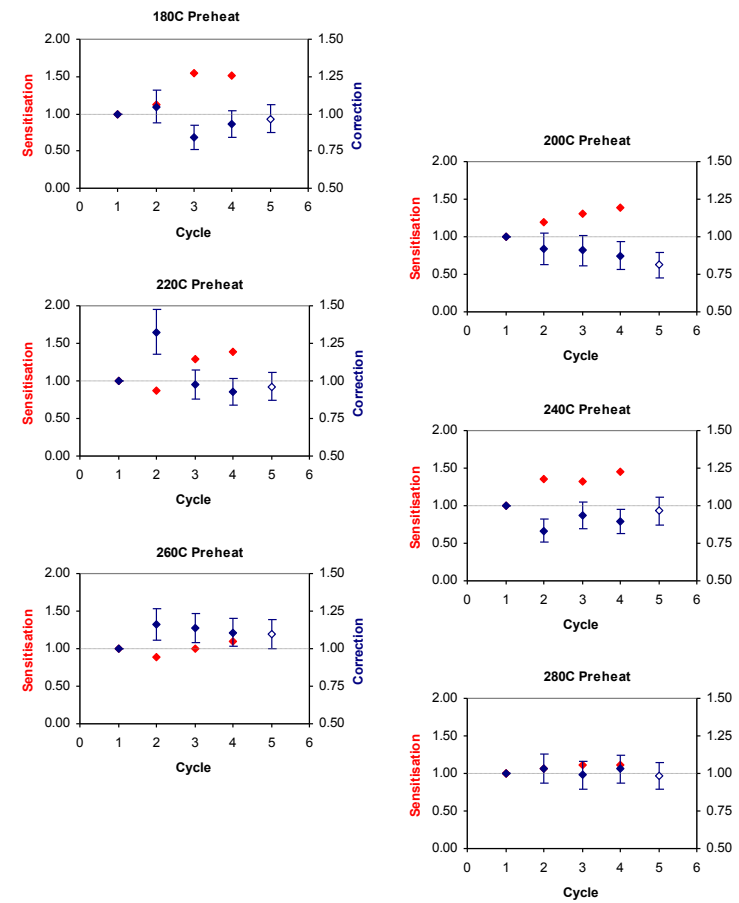


Fig. 3 D_e Preheat Dependence

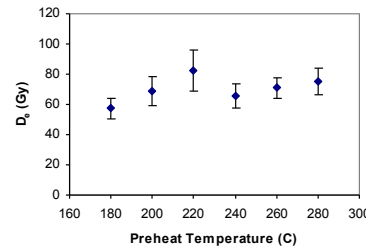


Fig. 4 Dose Recovery

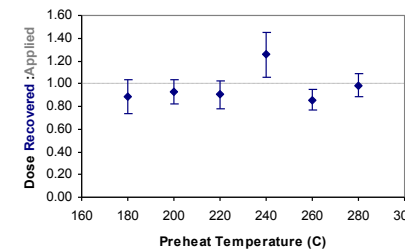


Fig. 5 Inter-aliquot D_e distribution

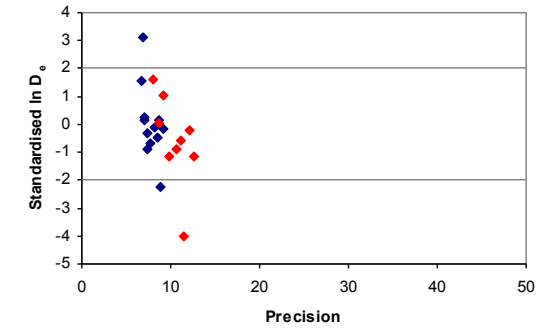


Fig. 6 Signal Analysis

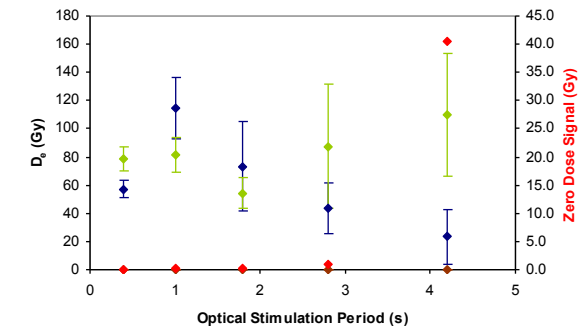


Fig. 7 U Decay Activity

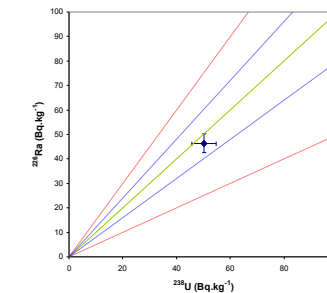
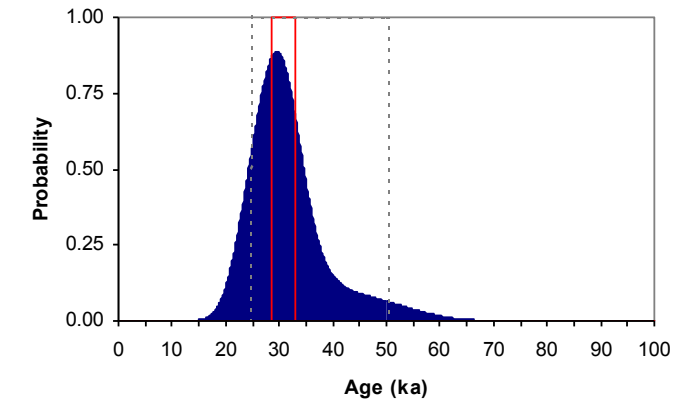


Fig. 8 Age Range



Sample: GL08067

APPENDIX 3: TECHNICAL DATA FOR SAMPLE GL08068

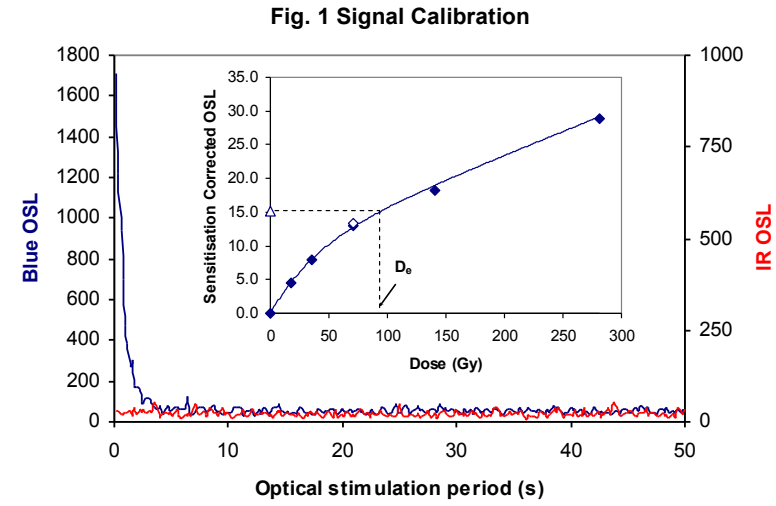


Fig. 1 Signal Calibration Natural blue and laboratory-induced infrared (IR) OSL signals. Detectable IR signal decays are diagnostic of feldspar contamination. Inset, the natural blue OSL signal (open triangle) of each aliquot is calibrated against known laboratory doses to yield equivalent dose (D_e) values. Where D_e values are >100 Gy, a log-linear plot of dose response is shown; D_e can be confidently interpolated if signal response increases with dose.

Fig. 2 Irradiation-Preheat Cycling The acquisition of D_e values is necessarily predicated upon thermal treatment of aliquots succeeding environmental and laboratory irradiation. Repeated irradiation and thermal treatment results in aliquot sensitisation, rendering calibration of the natural signal inaccurate. This sensitisation can be monitored and corrected for. The accuracy of correction can be preheat dependent; irradiation-preheat cycling quantifies this dependence for laboratory-induced signals, examining the reproducibility of corrected OSL resultant of repeat laboratory doses. The significance of feldspar contamination can be quantified by measuring the post-IR blue repeat ratio (open symbol).

Fig. 3 D_e Preheat Dependence Quantifies the combined effects of thermal transfer and sensitisation on the natural signal. Insignificant adjustment in D_e may reflect limited influence of these effects

Fig. 4 Dose Recovery Attempts to replicate the above diagnostic, yet provide improved resolution of thermal effects through removal of variability induced by heterogeneous dose absorption in the environment and using a precise lab dose to simulate natural dose. Based on this and preceding data an appropriate thermal treatment is selected to refine the final D_e value.

Fig. 5 Inter-aliquot D_e distribution Provides a measure of inter-aliquot statistical concordance in D_e values derived from natural and laboratory irradiation. Discordant data (those points lying beyond ± 2 standardised $\ln D_e$) reflects heterogeneous dose absorption and/or inaccuracies in calibration.

Fig. 6 Signal Analysis Statistically significant increase in natural D_e value with signal stimulation period is indicative of a partially-bleached signal, provided a significant increase in D_e results from simulated partial bleaching along with insignificant adjustment in D_e for simulated zero and full bleach conditions. Ages from such samples are considered maximum estimates.

Fig. 7 U Activity Statistical concordance (equilibrium) in the activities of the daughter radioisotope ^{226}Ra with its parent ^{238}U may signify the temporal stability of D_e emissions from these chains. Significant differences (disequilibrium; $>50\%$) in activity indicate addition or removal of isotopes creating a time-dependent shift in D_e values and increased uncertainty in the accuracy of age estimates. 20% disequilibrium marker is also shown.

Fig. 8 Age Range The mean age range provides an estimate of sediment burial period based on mean D_e and D_e values with associated analytical uncertainties. The probability distribution indicates the inter-aliquot variability in age. The maximum influence of temporal variations in D_e forced by minima-maxima variation in moisture content and overburden thickness may prove instructive where there is uncertainty in these parameters, however the combined extremes represented should not be construed as preferred age estimates.

Fig. 2 Irradiation-Preheat Cycling

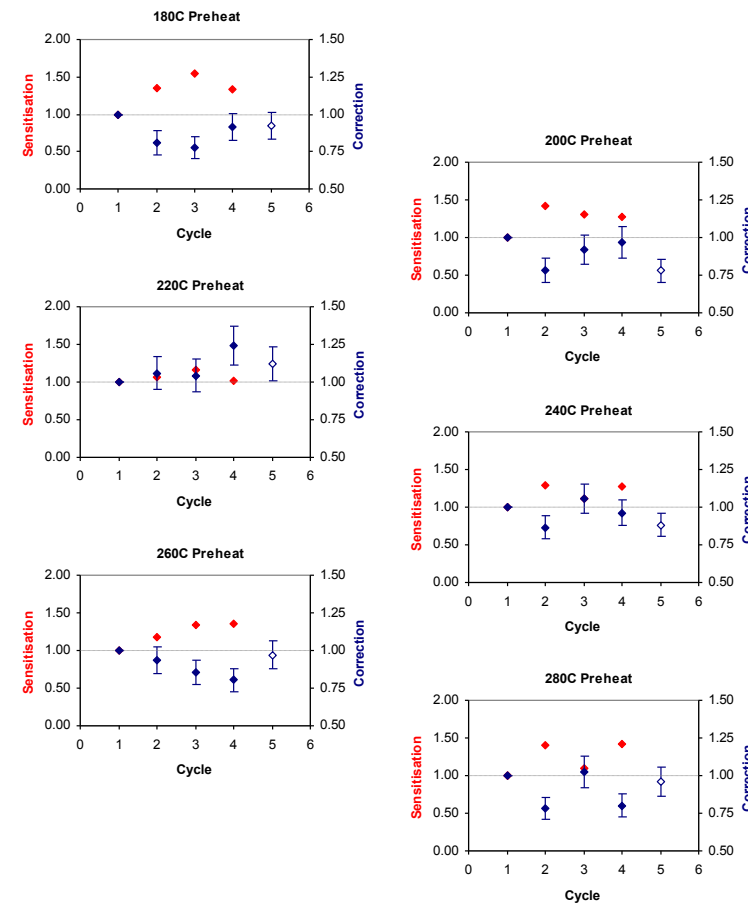


Fig. 3 D_e Preheat Dependence

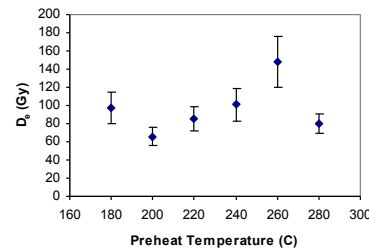


Fig. 4 Dose Recovery

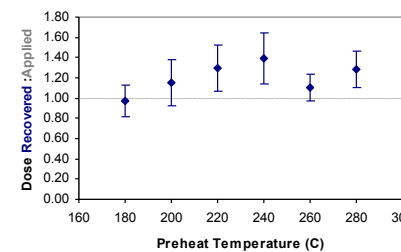


Fig. 5 Inter-aliquot D_e distribution

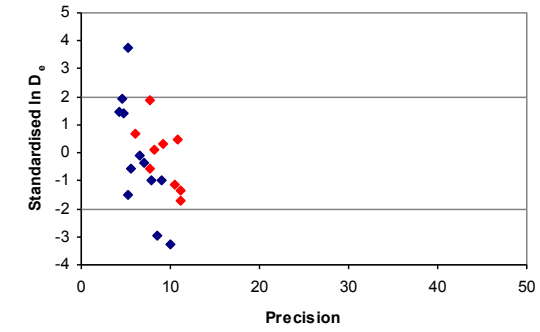


Fig. 6 Signal Analysis

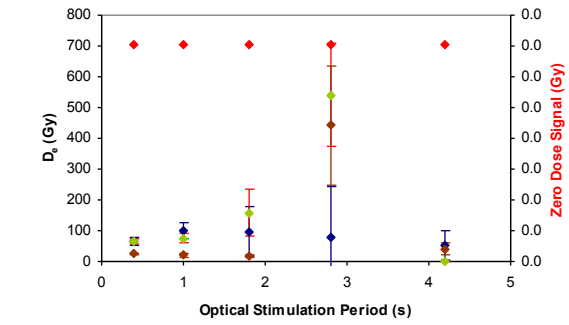


Fig. 7 U Decay Activity

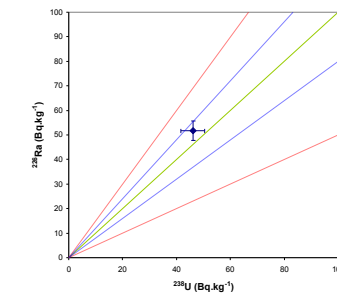
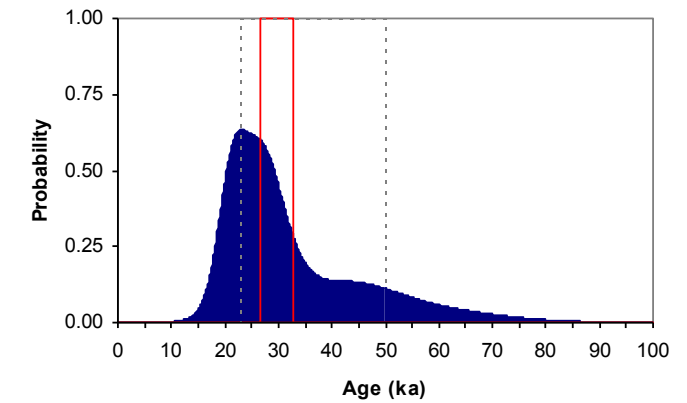


Fig. 8 Age Range



Sample: GL08068



ENGLISH HERITAGE RESEARCH DEPARTMENT

English Heritage undertakes and commissions research into the historic environment, and the issues that affect its condition and survival, in order to provide the understanding necessary for informed policy and decision making, for sustainable management, and to promote the widest access, appreciation and enjoyment of our heritage.

The Research Department provides English Heritage with this capacity in the fields of buildings history, archaeology, and landscape history. It brings together seven teams with complementary investigative and analytical skills to provide integrated research expertise across the range of the historic environment. These are:

- * Aerial Survey and Investigation*
- * Archaeological Projects (excavation)*
- * Archaeological Science*
- * Archaeological Survey and Investigation (landscape analysis)*
- * Architectural Investigation*
- * Imaging, Graphics and Survey (including measured and metric survey, and photography)*
- * Survey of London*

The Research Department undertakes a wide range of investigative and analytical projects, and provides quality assurance and management support for externally-commissioned research. We aim for innovative work of the highest quality which will set agendas and standards for the historic environment sector. In support of this, and to build capacity and promote best practice in the sector, we also publish guidance and provide advice and training. We support outreach and education activities and build these in to our projects and programmes wherever possible.

We make the results of our work available through the Research Department Report Series, and through journal publications and monographs. Our publication Research News, which appears three times a year, aims to keep our partners within and outside English Heritage up-to-date with our projects and activities. A full list of Research Department Reports, with abstracts and information on how to obtain copies, may be found on www.english-heritage.org.uk/researchreports

For further information visit www.english-heritage.org.uk

